Published in final edited form as:
J Biomech. 2009 March 11; 42(4): 491–497. doi:10.1016/j.jbiomech.2008.11.016.

Progressive post-yield behavior of human cortical bone in compression for middle-aged and elderly groups

Huijie Leng[a], **X. Neil Dong**[b], and **Xiaodu Wang**[b,*]

[a]Department of Orthopaedics, Peking University Third Hospital, Beijing 100191, China

[b]Department of Mechanical Engineering, University of Texas at San Antonio, One UTSA Circle, San Antonio, TX 78249, USA

Abstract

In this study, a progressive loading regimen (load–dwell–unloading–dwell–reloading) was applied on bone samples to examine the compressive post-yield response of bone at increasing strain levels. Cortical bone specimens from human tibiae of two age groups (middle-aged group: 53±2 years, 4 females and 4 males, elderly group: 83±6 years, 4 females and 4 males) were loaded in compression using the progressive loading scheme. Modulus degradation, plastic deformation, viscous response, and energy dissipation of bone during post-yield deformation were assessed. Although initial modulus was not significantly different between the two age groups, the degradation of modulus with the applied strain in the elderly group was faster than in the middle-aged group. The modulus loss (or microdamage accumulation) of bone occurred prior to plastic deformation. Plastic strain had a similar linear relationship with the applied strain for both middle-aged and the elderly group although middle-aged bone yielded at a greater strain. The viscoelastic time constant changed similarly with increasing strain for the two groups, whereas a higher magnitude of stress relaxation was observed in the middle-aged group. Energy dissipation was investigated through three pathways: elastic release strain energy, hysteresis energy, and plastic strain energy. The middle-aged group had significantly greater capacity of energy dissipation than the elderly group in all three pathways. The information obtained may provide important insights in age-related effects on bone fragility.

Keywords

Cortical bone; Compression; Post-yield; Aging; Energy dissipation

1. Introduction

Bone quality is determined by a combination of factors that directly contribute to the fragility of the tissue (Bouxsein, 2003; Felsenberg and Boonen, 2005; Hernandez and Keaveny, 2006). Toughness (i.e., total energy dissipation until failure) has served as a key measure of bone quality (Wang and Puram, 2004). Since the major part of strain energy is dissipated through the post-yield deformation of bone, the post-yield behavior actually dominates the tissue toughness (Courtney et al., 1996; Fondrk et al., 1999).

*Corresponding author. Tel.: +1 210 458 5565; fax: +1 210 458 6504. xiaodu.wang@utsa.edu (X. Wang).

Conflict of interest statement

Each author in this manuscript does not have and will not receive benefits in any form from a commercial party related directly or indirectly to the content in this manuscript. The authors declare that they have no competing financial interests.

The post-yield behavior of bone is usually associated with microdamage accumulation (Forwood and Parker, 1989; Burr et al., 1997, 1998; Fazzalari et al., 1998a, [b]; Norman et al., 1998; Reilly and Currey, 1999; Timlin et al., 2000; Akkus and Rimnac, 2001), viscoelastic responses (Bredbenner and Davy, 2006; Joo et al., 2007; Yeni et al., 2007), and plastic deformation (Fondrk et al., 1988). For instance, yielding coincides with the formation of damage in bone (Zioupos et al., 1994), and the induced damages may lead to an elevated viscoelastic response of bone (Yeni et al., 2007). In addition, microdamage accumulation plays a significant role in energy dissipation in both fatigue and monotonic fractures of bone (Schaffler et al., 1995; Burr et al., 1997; Jepsen and Davy, 1997; Martin et al., 1997; Fazzalari et al., 1998a, [b]; Norman et al., 1998; Vashishth et al., 1997, 2003; Zioupos, 2001).

Most previous studies employed the monotonic loading mode to investigate the mechanical behavior of bone (Reilly and Burstein, 1975; Burstein et al., 1976; Carter and Hayes, 1976; Walsh and Guzelsu, 1994; Les et al., 2002; Currey, 2004), except for a few studies that employed diagnostic loading cycles to around 1% strain in tension (Courtney et al., 1996; Jepsen and Davy, 1997; Joo et al., 2007) and in torsion (Jepsen et al., 1999)to investigate the behavior of bone after yielding. Moreover, the fatigue-induced microdamage accumulation was also studied in different loading modes (Martin et al., 1997; Winwood et al., 2006). Although those studies provided useful information about the mechanical events, little is known about the evolution of the tissue behavior during the post-yield deformation of bone.

Recently, we developed a novel progressive cyclic loading protocol to investigate the evolution of the post-yield behavior of bone in tension (Nyman et al., 2007; Wang and Nyman, 2007). In the present study, the same technique was used to examine the post-yield behavior of bone in compression. The hypothesis of this study is that the capacity of bone to dissipate energy in the post-yield deformation in compression is significantly lower for elderly bone than middle-aged bone.

2. Materials and methods

2.1. Specimen preparation

Sixteen human cadaveric tibiae were obtained from the Willed Body Program (The University of Texas Southwestern Medical Center at Dallas, TX) with the stipulation that the donors had no known bone disease. The specimens were divided into two age groups: middle-aged (53 ± 2 years) and elderly (83 ± 6 years) groups. The former had 4 female donors of 53, 54, 54, and 56 years and 4 male donors of 55, 51, 51, and 52 years, while the latter consisted of 4 female donors of 84, 88, 88, and 90 years and 4 male donors of 72, 76, 79, and 87 years. A cylindrical bone specimen with a diameter of 3 mm and a height of 5 mm was prepared each from the anterior quadrant of the diaphyseal tibiae in the longitudinal direction (Fig. 1). It was ensured by staining in a pilot study that little microdamages were induced during the preparation process. All specimens were wrapped in gauze, soaked in phosphate-buffered saline (PBS), and stored at −20 °C until testing.

2.2. Mechanical testing

Prior to mechanical testing, all the specimens were thawed at room temperature for around 3 h in PBS. The bone specimen was tested in compression at room temperature using a load–dwell–unload–dwell–reload scheme on a MTS mechanical testing system (Insight 5000, MTS, Eden Prairie, MN), with an extensometer of 3 mm gage attached (Fig. 1). Based on a physiologically relevant strain rate 0.001/s (Courtney et al., 1996), the loading rate was set as 0.005 mm/s for displacement control in the loading/reloading process and 5 N/s for load control in the unloading process. In the first cycle, each bone specimen was preloaded to 20 N to ensure a proper engagement between the specimen and the loading fixture. Then, the

specimen was loaded to 0.03 mm of crosshead displacement, held at the strain level under displacement control for 30s (stress relaxation dwell), unloaded to 20 N, and held at 20 N under load control for 30 s (strain relaxation dwell). Thirty seconds were long enough to reach equilibrium for the first cycle because little viscous responses were present at the strain level. In the succeeding cycles, the same loading procedure was repeated with a series of sequential increment of crosshead displacement: 0.05, 0.06, 0.08, 0.1, 0.11, 0.12, 0.13, 0.15,0.17, 0.19,0.22, 0.25, and 2.0 mm in order to catch the evolution of tissue behavior with the increasing post-yield deformation. The dwelling time for both load and displacement control was extended to 2 min to ensure that full equilibrium was reached during the dwells. Finally, the test was stopped at either final failure of the specimen or the travel limit of the extensometer. The test specimen was kept wet by continuously dripping PBS onto a paper tissue that was wrapped around the gage region of the specimen.

Additionally, another cylindrical bone sample from each donor was prepared and monotonically loaded in compression at 0.005 mm/s to final failure or the travel limit of the extensometer. The monotonic stress–strain curve was compared with the progressive behavior of bone obtained from the cyclic loading scheme.

2.3. Microdamage detection

After mechanical testing, each specimen was bulk strained following a well-established staining protocol for examining microdamage in bone (Burr and Hooser, 1995). The stained specimen was embedded in methylmethacrylate (Kolmount, Vernon-Benshoff Company, Albany, NY) and sectioned longitudinally using a diamond saw (Isomet 2000, Buehler, Lake Bluff, IL). The longitudinal bone section was ground and polished to a thickness of 100 μm with successive grits of sand paper. The morphology of microdamages in bone was examined at × 100 magnification under epi-fluorescence microscopy (Leica DM5500B, Leica Microsystems).

2.4. Quantification of mechanical properties

Mechanical properties of each specimen were quantified at each progressive-strain level (Fig. 2). The initial modulus (E_0) was estimated at the first loading cycle. The instantaneous modulus (E_i) at each subsequent loading cycle was estimated as the slope of a line between the points at the end of stress relaxation dwelling before unloading and at the end of anelastic deformation dwelling after unloading (Fig. 2). The experimental data of applied strain vs. elastic modulus were curve fitted using an exponential equation (Table Curve 2D, Systat Software, San Jose, CA)

$$E_i = E_0 e^{-m(\varepsilon_i - \varepsilon_0)} \quad (1)$$

Here m defines the sensitivity of bone to damage accumulation. A higher value of m means faster stiffness loss. ε_i is the applied strain, and ε_0 is the strain level at which the initial modulus was estimated.

The plastic strain (ε_p) was determined as the residual strain at the end of each load–dwell–unload–dwell cycle (i.e., the end of strain relaxation dwell). The yield strain (ε_y) was determined by linearly fitting the plastic strain vs. applied strain curve as shown in Fig. 3a. The yield stress (ε_y) was defined as the stress corresponding to the yield strain. The ultimate stress (ε_{ult}) was defined as the maximum stress in the stress–strain curve.

The viscoelastic time constant (τ) was estimated by fitting the stress–time curve during the stress relaxation dwelling using an exponential equation

$$\Delta\sigma=\Delta\sigma_0 e^{-t/\tau}+A\ t+B \quad (2)$$

where $\Delta\sigma_0$ is the magnitude of total stress relaxation and τ is viscoelastic time constant. The linear terms ($At+B$) were added based on the experimental observation (Fig. 3b).

Energy dissipation was partitioned into three pathways in this study (i.e., elastic release strain energy: *Uer*, hysteresis energy: *Uhy*, and plastic strain energy: *Upl*) (Nyman et al., 2007; Wang and Nyman, 2007). These energy dissipation terms were the areas between or under the loading/unloading curves (Fig. 2). The elastic release strain energy was defined as the area under the unloading curve minus the triangular area due to the nominal elastic recovery at the initial elastic modulus. The hysteresis energy was the area between the loading and unloading curves of each cycle. The plastic strain energy was the cumulative area (*Um*) minus the elastic release strain energy (Fig. 2).

All aforementioned properties were calculated using a custom MATLAB script (Mathworks, Natick, MA). Initial modulus, yield strain, yield stress, and maximum stress were compared between the two age groups using a Student's *t*-test (Table 1). The differences of the linearly fitted slopes of plastic strain, plastic strain energy, elastic release strain energy, and hysteresis energy between the two age groups were also determined using the analysis of covariance (ANCOVA). The significance was considered only if $p < 0.05$.

3. Results

Overall, the cyclic loading with relaxation insertions successfully captured the evolution of bone behavior from pre- to post-yielding. With increasing strain, stress increased linearly in the elastic region, then reached to the maximum level (σ_{ult}), and then decreased gradually. The "envelop" of strain–stress curve from the cyclic loading was able to follow the trend of monotonic loading curve (Fig. 4).

The bulk failure behavior of bone in compression could be categorized by oblique fractures through both ends of the specimens and cone-shaped fractures in the middle of cylindrical specimens (Fig. 5). As to the bulk mechanical properties of bone, statistical analysis showed that the initial modulus (E_0) and the strength (σ_{ult}) were not significantly different between the middle-aged and elderly groups (Table 1). However, the middle-aged bone specimens demonstrated higher yield strain (ε_y) and yield stress (σ_y) than those from the elderly ones ($p<0.05$) (Table 1).

The elastic modulus of bone dropped immediately after the first loading cycle and decreased more than 50% of the initial modulus at about 1% strain for both the age groups. The nonlinear regression of the applied strain versus the instantaneous elastic modulus demonstrated a relationship of $E_i = 18.8\ e^{-52.7(\varepsilon_i-0.0012)}$ for the middle-aged group and $E_i = 19.0\ e^{-64.3(\varepsilon_i-0.002)}$ for the elderly group (Fig. 6). The elderly group had a higher exponent ($m = 64.3$), suggesting that its modulus degradation was relatively faster than the middle-aged group.

The plastic strain (ε_p) increased linearly with respect to the applied strain for both the age groups (Fig. 7). ANCOVA results showed that there was no significant difference between the slopes from linear regression for the middle-aged and elderly groups ($p = 0.08$).

Viscous responses of bone were reflected in the viscoelastic time constant (τ) and the magnitude of stress relaxation ($\Delta\sigma_0$). Age-related difference was not observed in the viscoelastic time constant (Fig. 8), but was found in the magnitude of stress relaxation (Fig.

9). For both the age groups, the viscoelastic time constant dropped sharply with increasing strain until about 1%. Afterwards, the time constant leveled off and became a plateau (Fig. 8). The magnitude of stress relaxation first increased linearly with increasing strain, then reached to a peak value at a strain ranging between 1.0% and 1.2%, and finally became a plateau for both the age groups. However, the middle-aged bone specimens exhibited higher peak values at large strain levels compared with those of the elderly bone specimens (Fig. 9).

Age-related effects on the energy dissipation in bone were significant, showing significant increases in the amount of energy dissipation in all the three pathways. A linear relationship was observed between the plastic strain energy and applied strain after yielding of bone (Fig. 10). ANCOVA analyses showed that the slope of the curve was significantly higher for the middle-aged group than for the elderly group ($p<0.05$). On the other hand, the elastic release strain energy and hysteresis energy dissipations showed approximately bilinear relationship with the applied strain (Figs. 11 and 12). Linear regressions were also applied to elastic release strain energy and hysteresis energy versus applied strain in the region with strain more than 1%. In all the three pathways, middle-aged bone dissipated significantly more energy than elderly bone ($p<0.05$).

By plotting the plastic strain with respect to the percent of modulus loss, it was indicated that the plastic deformation was not noticeable until more than 30% modulus loss was reached (Fig. 13).

4. Discussion

Using the novel progressive loading technique, we investigated both bulk and micro/ultrastructural properties during the post-yield deformation of bone in compression. The results of this study indicate that except for the yield stress and strain (i.e., σ_y and ε_y), there were no significant differences in the initial modulus (E_0) and the strength (σ_{ult}) of bone between the middle-aged and elderly groups. Obviously, these bulk mechanical properties provided very limited information on the failure behavior of bone in compression. However, examining the evolution of bone behavior after yielding (i.e., modulus loss, plastic deformation, viscous response, and energy dissipation) shed more light on the underlying mechanism of bone failure.

The modulus loss has been reported to be directly related to the increased density of microdamage accumulated during the post-yield deformation of bone (Carter and Hayes, 1977; Zioupos and Currey, 1994; Schaffler et al., 1995; Burr et al., 1998). It is conceivable that the elastic release strain energy is dissipated through the formation of new damage surfaces by microdamage accumulation (Fondrk et al., 1999). Thus, the capacity of bone to dissipate such energy would depend on how much surface energy could be released from the new damage surfaces (i.e., surface energy density) and how big the total area of such surfaces. The results of this study indicate that elderly bone exhibited a faster modulus loss (i.e., greater values of m), but less elastic release strain energy dissipation than middle-aged bone (Figs. 6 and 11). This suggests that the surface energy density for new damage surfaces formed in the elderly bone is less than that of the middle-aged bone, implying that the elderly bone behaves in a more brittle way in generating microdamage.

Linear relationships of the plastic deformation (ε_p) and plastic strain energy dissipation (Upl) with increasing strain were observed in compression. This supports the speculation that in compression a linear mechanism may exists in the plastic deformation of bone. However, with similar plastic strains the middle-aged dissipated more plastic strain energy than the elderly bone, indicating that the middle-aged bone may require more energy to

deform plastically than the elderly bone. Since the mechanism of the plastic deformation in bone is still unclear, this issue needs further investigations.

Another difference between the middle-age and elderly bone is reflected in the hysteresis energy dissipation. The middle-aged bone was able to dissipate more hysteresis energy than the elderly bone after the viscous response saturated at about 1% strain (Fig. 12). Since the hysteresis energy dissipation is determined by the viscoelastic behavior of bone (Doubal et al., 2004), age-related effects on the capacity of the tissue to dissipate hysteresis energy would be manifested in changes of such properties. It is noteworthy that the difference between the middle-aged and elderly groups is discernable only in the magnitude of stress relaxation (Fig. 9), but not in the time constant (Fig. 8). One possible explanation is that age-related changes may alter the behavior of the collagen phase, which may lead to a reduced tissue capacity for stress relaxation and consequently reduce the hysteresis energy dissipation in bone.

One interesting observation of this study is that the modulus loss in compression occurs much earlier than yielding of bone (Fig. 6 and Table 1). The modulus loss begins at a much smaller strain (about 0.2%) than the yield strain (0.82% and 0.71% for the middle-aged and elderly groups, respectively). Some previous studies have reported that yielding is initiated by microdamage formation (Zioupos et al., 1994) and may occur simultaneously with microdamage accumulation in trabecular bone samples (Morgan et al., 2005). However, our results indicate that in compression the microdamage accumulation in bone could add up to the 30% of modulus loss before the plastic deformation starts to take place. The disparity between our results and the previous ones may be largely due to the differences in the type and configuration of specimens (e.g., cortical vs. trabecular bone) as well as loading conditions (e.g., fatigue vs. progressive loading scheme). For example, neither fatigue nor creep would have significant effects on our progressive loading tests. However, both fatigue and creep were involved in the tests of the other studies. Such a difference may lead to the plastic deformation induced by creep even at small strain levels.

Among the two failure modes (i.e., oblique and butterfly shaped) observed in this study (Fig. 4), oblique-shaped failure was more dominant in the tests. The microdamage formation in bone in compression is characterized by cross-hatched cracks with an angle close to the direction of maximum shear stress for both age groups (Fig. 14). This suggests that shear is the dominant mechanism of microdamage formation in bone in compression. Interestingly, it is quite similar to slip lines formed during plastic deformation of ductile metals.

There are several limitations for this study. One is the limited number of samples ($N = 8$), which may lessen the power of statistical analyses to detect the differences between the age groups. To address this issue, a power analysis of experimental data was performed and a power of 0.8 was obtained for the sample size ($N = 8$) to detect the differences with an effective size of 1.65 if $\alpha < 0.05$. Using the mean and standard deviation of the experimental data, the detectable difference was estimated to be about 11%. Another limitation is the age range of bone samples (middle-aged vs. elderly). Thus, the conclusion of this study would be restricted to the age range. Finally, it is worth to mention that this study only examined the post-yield behavior of bone within a strain range of less than 5% because the final failure was difficult to define. The same difficulty was also faced by other researchers (Reilly and Burstein, 1975). Thus, the information provided by this study is mainly in the post-yield region excluding the behavior at the final failure of bone.

In summary, age-related changes have been found in elastic modulus degradation, yielding behavior, stress relaxation, and energy dissipation of bone in compression. Micro/ultrastructural changes in bone constituents may be responsible for the altered mechanical

behavior of bone. The outcome of this study may shed lights on the mechanisms of the age-related bone fragility.

Acknowledgments

This work was supported by a NIH/NIA grant (R01AG022044).

References

Akkus O, Rimnac CM. Cortical bone tissue resists fatigue fracture by deceleration and arrest of microcrack growth. Journal of Biomechanics 2001;34:757–764. [PubMed: 11470113]

Bouxsein ML. Bone quality: where do we go from here? Osteoporosis International 2003;14:S118–S127. [PubMed: 14504716]

Bredbenner TL, Davy DT. The effect of damage on the viscoelastic behavior of human vertebral trabecular bone. Journal of Biomechanical Engineering 2006;128:473–480. [PubMed: 16813438]

Burr DB, Hooser M. Alterations to the en bloc basic fuchsin staining protocol for the demonstration of microdamage produced in vivo. Bone 1995;17:431–433. [PubMed: 8573418]

Burr DB, Forwood MR, Fyhrie DP, Martin RB, Schaffler MB, Turner CH. Bone microdamage and skeletal fragility in osteoporotic and stress fractures. Journal of Bone and Mineral Research 1997;12:6–15. [PubMed: 9240720]

Burr DB, Turner CH, Naick P, Forwood MR, Ambrosius W, Hasan MS, Pidaparti R. Does microdamage accumulation affect the mechanical properties of bone? Journal of Biomechanics 1998;31:337–345. [PubMed: 9672087]

Burstein AH, Reilly DT, Martens M. Aging of bone tissue: mechanical properties. Journal of Bone and Joint Surgery, American 1976;58:82–86.

Carter DR, Hayes WC. Bone compressive strength: the influence of density and strain rate. Science 1976;194:1174–1176. [PubMed: 996549]

Carter DR, Hayes WC. Compact bone fatigue damage—I. Residual strength and stiffness. Journal of Biomechanics 1977;10:325–337. [PubMed: 893471]

Courtney AC, Hayes WC, Gibson LJ. Age-related differences in post-yield damage in human cortical bone. Experiment and model. Journal of Biome-chanics 1996;29:1463–1471.

Currey JD. Tensile yield in compact bone is determined by strain, post-yield behaviour by mineral content. Journal of Biomechanics 2004;37:549–556. [PubMed: 14996567]

Doubal S, Klemera K, Semeckay V, Lamka J, Kucharovaa M. Non-linear mechanical behavior of visco-elastic biological structure measurements and models. Acta Medica (Hradec Kraalovae)/ Universitas Carolina, Facultas Medica Hradec Kraalovae 2004;47:297–300.

Fazzalari NL, Forwood MR, Manthey BA, Smith K, Kolesik P. Three-dimensional confocal images of microdamage in cancellous bone. Bone 1998a;23:373–378. [PubMed: 9763150]

Fazzalari NL, Forwood MR, Smith K, Manthey BA, Herreen P. Assessment of cancellous bone quality in severe osteoarthrosis: bone mineral density, mechanics, and microdamage. Bone 1998b;22:381–388. [PubMed: 9556139]

Felsenberg D, Boonen S. The bone quality framework: determinants of bone strength and their interrelationships, and implications for osteoporosis management. Clinical Therapeutics 2005;27:1–11. [PubMed: 15763602]

Fondrk M, Bahniuk E, Davy DT, Michaels C. Some viscoplastic characteristics of bovine and human cortical bone. Journal of Biomechanics 1988;21:623–630. [PubMed: 3170617]

Fondrk MT, Bahniuk EH, Davy DT. A damage model for nonlinear tensile behavior of cortical bone. Journal of Biomechanical Engineering 1999;121:533–541. [PubMed: 10529922]

Forwood MR, Parker AW. Microdamage in response to repetitive torsional loading in the rat tibia. Calcified Tissue International 1989;451:47–53. [PubMed: 2504464]

Hernandez CJ, Keaveny TM. A biomechanical perspective on bone quality. Bone 2006;39:1173–1181. [PubMed: 16876493]

Jepsen KJ, Davy DT. Comparison of damage accumulation measures in human cortical bone. Journal of Biomechanics 1997;30:891–894. [PubMed: 9302611]

Jepsen KJ, Davy DT, Krzypow DJ. The role of the lamellar interface during torsional yielding of human cortical bone. Journal of Biomechanics 1999;32:303–310. [PubMed: 10093030]

Joo W, Jepsen KJ, Davy DT. The effect of recovery time and test conditions on viscoelastic measures of tensile damage in cortical bone. Journal of Biomechanics 2007;40:2731–2737. [PubMed: 17412349]

Les CM, Stover SM, Keyak JH, Taylor KT, Kaneps AJ. Stiff and strong compressive properties are associated with brittle post-yield behavior in equine compact bone material. Journal of Orthopaedic Research 2002;20:607–614. [PubMed: 12038638]

Martin RB, Gibson VA, Stover SM, Gibeling JC, Griffin LV. Residual strength of equine bone is not reduced by intense fatigue loading: implications for stress fracture. Journal of Biomechanics 1997;30:109–114. [PubMed: 9001930]

Morgan EF, Yeh OC, Keaveny TM. Damage in trabecular bone at small strains. European Journal of Morphology 2005;42:13–21. [PubMed: 16123020]

Norman TL, Yeni YN, Brown CU, Wang Z. Influence of microdamage on fracture toughness of the human femur and tibia. Bone 1998;23:303–306. [PubMed: 9737354]

Nyman JS, Roy A, Tyler JH, Acuna RL, Gayle HJ, Wang X. Age-relatesfactors affecting the postyield energy dissipation of human cortical bone. Journal of Orthopaedic Research 2007;25:646–655. [PubMed: 17266142]

Reilly DT, Burstein AH. The elastic and ultimate properties of compact bone tissue. Journal of Biomechanics 1975;8:393–405. [PubMed: 1206042]

Reilly GC, Currey JD. The development of microcracking and failure in bone depends on the loading mode to which it is adapted. Journal of Experimental Biology 1999;202(5):543–552. [PubMed: 9929457]

Schaffler MB, Choi K, Milgrom C. Aging and matrix microdamage accumulation in human compact bone. Bone 1995;17:521–525. [PubMed: 8835305]

Timlin JA, Garden A, Morris MD, Rajachar RM, Kohn DH. Raman spectroscopic imaging markers for fatigue-related microdamage in bovine bone. Analytical Chemistry 2000;72:2229–2236. [PubMed: 10845368]

Vashishth D, Behiri JC, Bonfield W. Crack growth resistance in cortical bone: concept of microcrack toughening. Journal of Biomechanics 1997;30:763–769. [PubMed: 9239560]

Vashishth D, Tanner KE, Bonfield W. Experimental validation of a microcracking-based toughening mechanism for cortical bone. Journal of Biomechanics 2003;36:121–124. [PubMed: 12485646]

Walsh WR, Guzelsu N. Compressive properties of cortical bone: mineral–organic interfacial bonding. Biomaterials 1994;15:137–145. [PubMed: 8011860]

Wang X, Nyman JS. A novel approach to assess post-yield energy dissipation of bone in tension. Journal of Biomechanics 2007;40:674–677. [PubMed: 16545820]

Wang X, Puram S. The toughness of cortical bone and its relationship with age. Annals of Biomedical Engineering 2004;32:123–135. [PubMed: 14964728]

Winwood K, Zioupos P, Currey JD, Cotton JR, Taylors M. Strain patterns during tensile, compressive, and shear fatigue of human cortical bone and implications for bone biomechanics. Journal of Biomedical Materials Research Part A 2006;79A:289–297. [PubMed: 16817209]

Yeni YN, Shaffer RR, Baker KC, Dong XN, Grimm MJ, Les CM, Fyhrie DP. The effect of yield damage on the viscoelastic properties of cortical bone tissue as measured by dynamic mechanical analysis. Journal of Biomedical Materials Research Part A 2007;82A:530–537. [PubMed: 17295254]

Zioupos P. Accumulation of in-vivo fatigue microdamage and its relation to biomechanical properties in ageing human cortical bone. Journal of Microscopy—Oxford 2001;201:270–278.

Zioupos P, Currey JD. The extent of microcracking and the morphology of microcracks in damaged bone. Journal of Materials Science 1994;29:978–986.

Zioupos P, Currey JD, Sedman AJ. An examination of the micromechanics of failure of bone and antler by acoustic emission tests and laser scanning confocal microscopy. Medical Engineering and Physics 1994;16:203–212. [PubMed: 8061906]

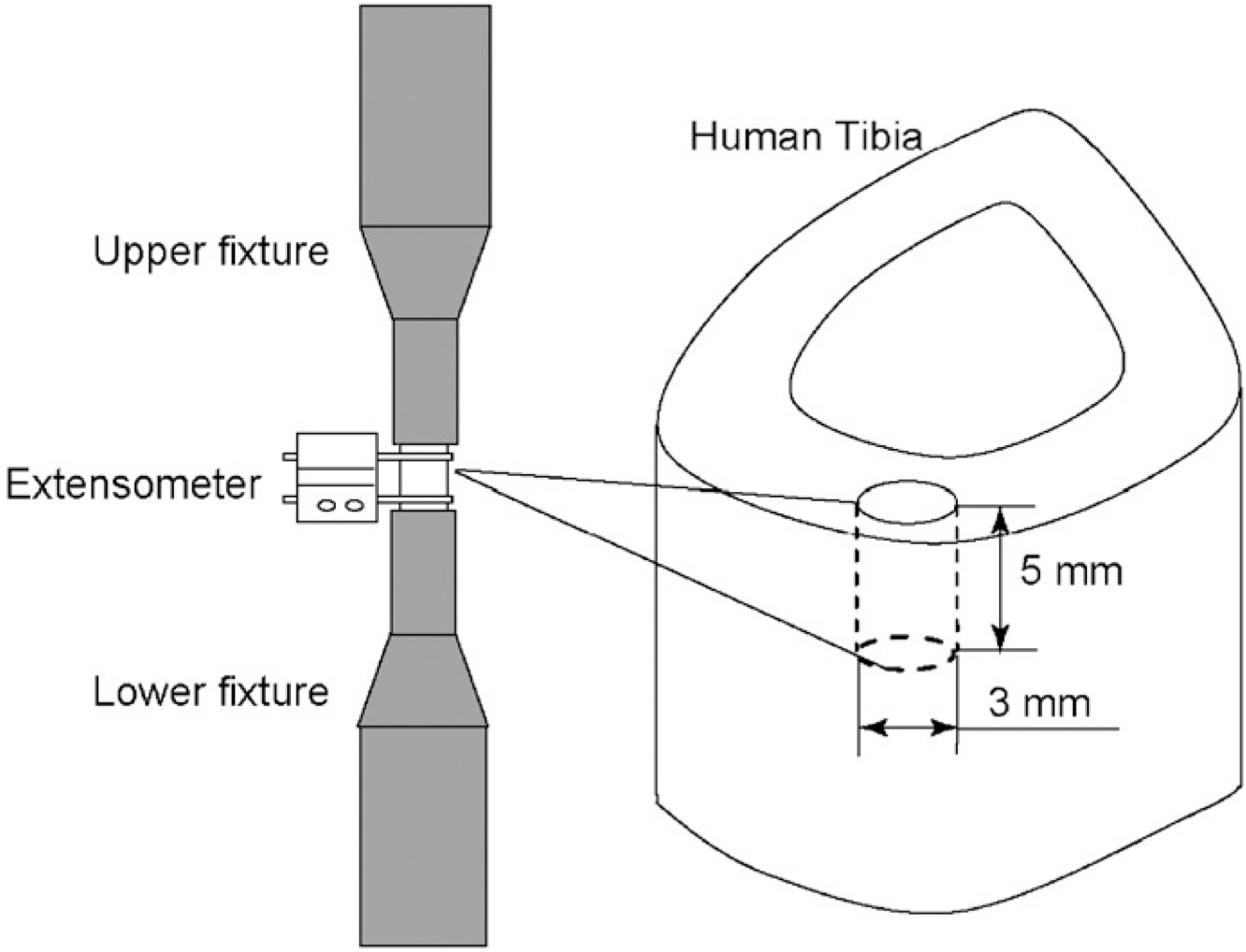

Fig. 1.
Schematic representation of specimen preparation and mechanical testing.

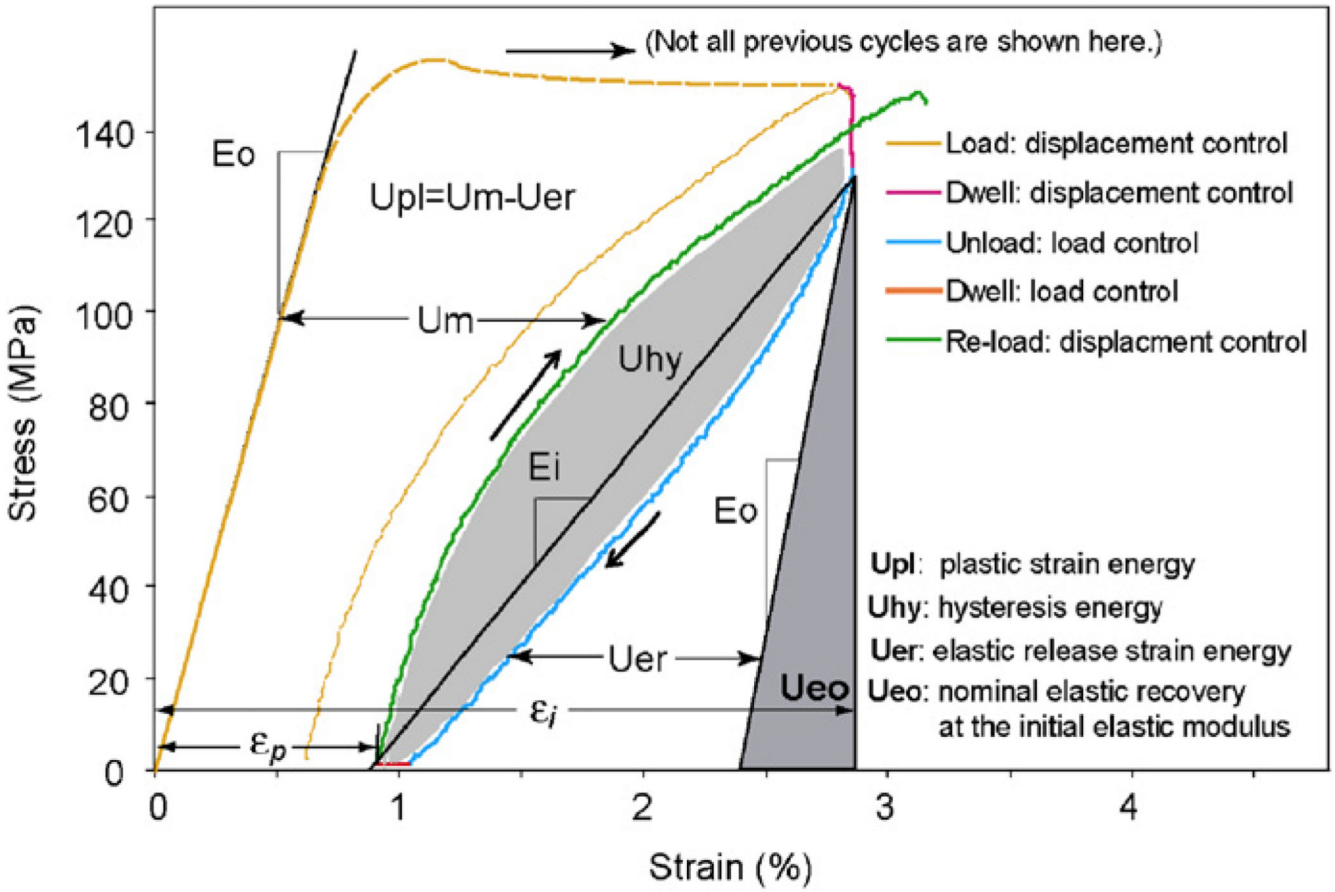

Fig. 2.
Illustration of methods for determining the mechanical properties of bone in each load–dwell–unload–dwell cycle during the progressive loading test.

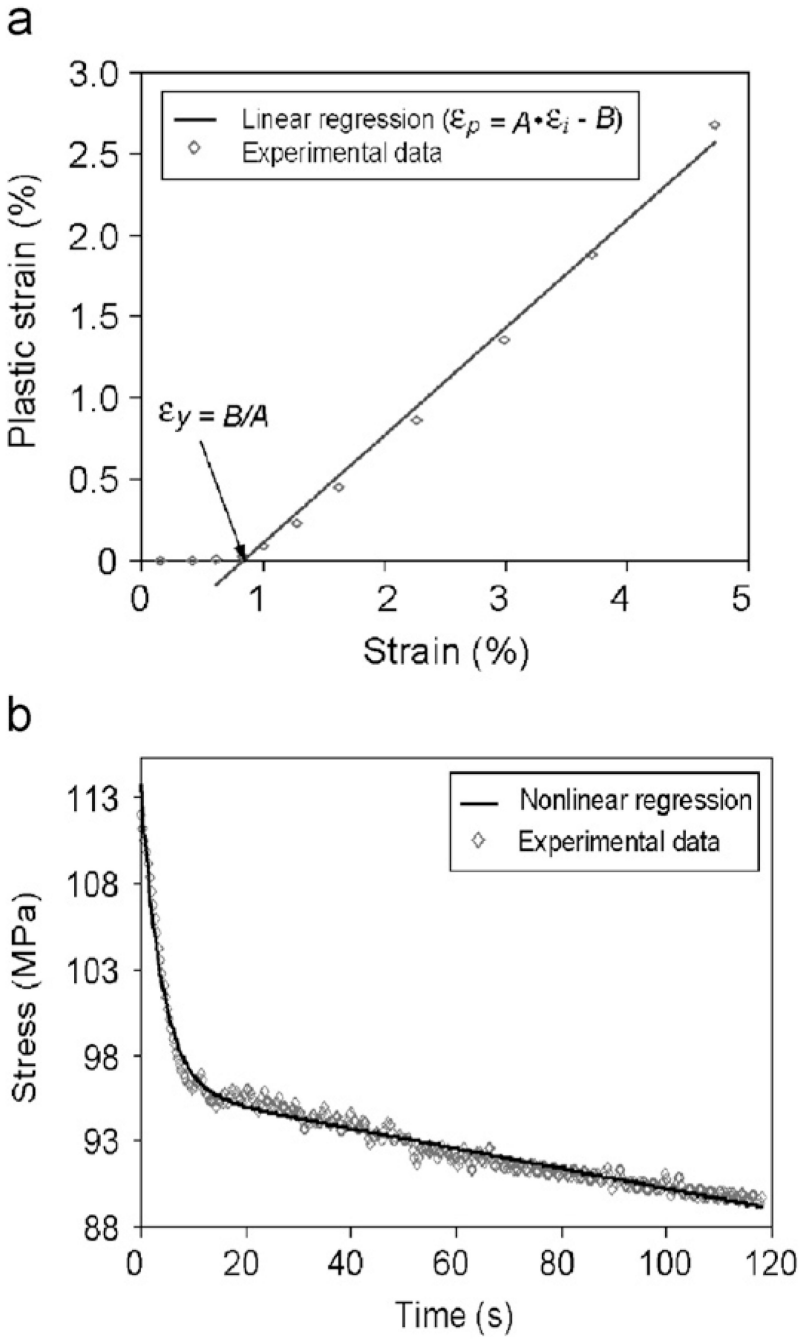

Fig. 3.

Methods for determination of the yield strain (ε_y) and viscoelastic time constant (τ). (a) Determination of yield strain (ε_y) based on a linear regression of the linear portion of the instantaneous strain (ε_i) and the plastic strain (ε_p) curve by making $\varepsilon_p = A\varepsilon_i - B = 0$ (i.e., $\varepsilon_y = B/A$); (b) determination of viscoelastic time constant (τ) based on an exponential equation fitting of the stress relaxation vs. time curve.

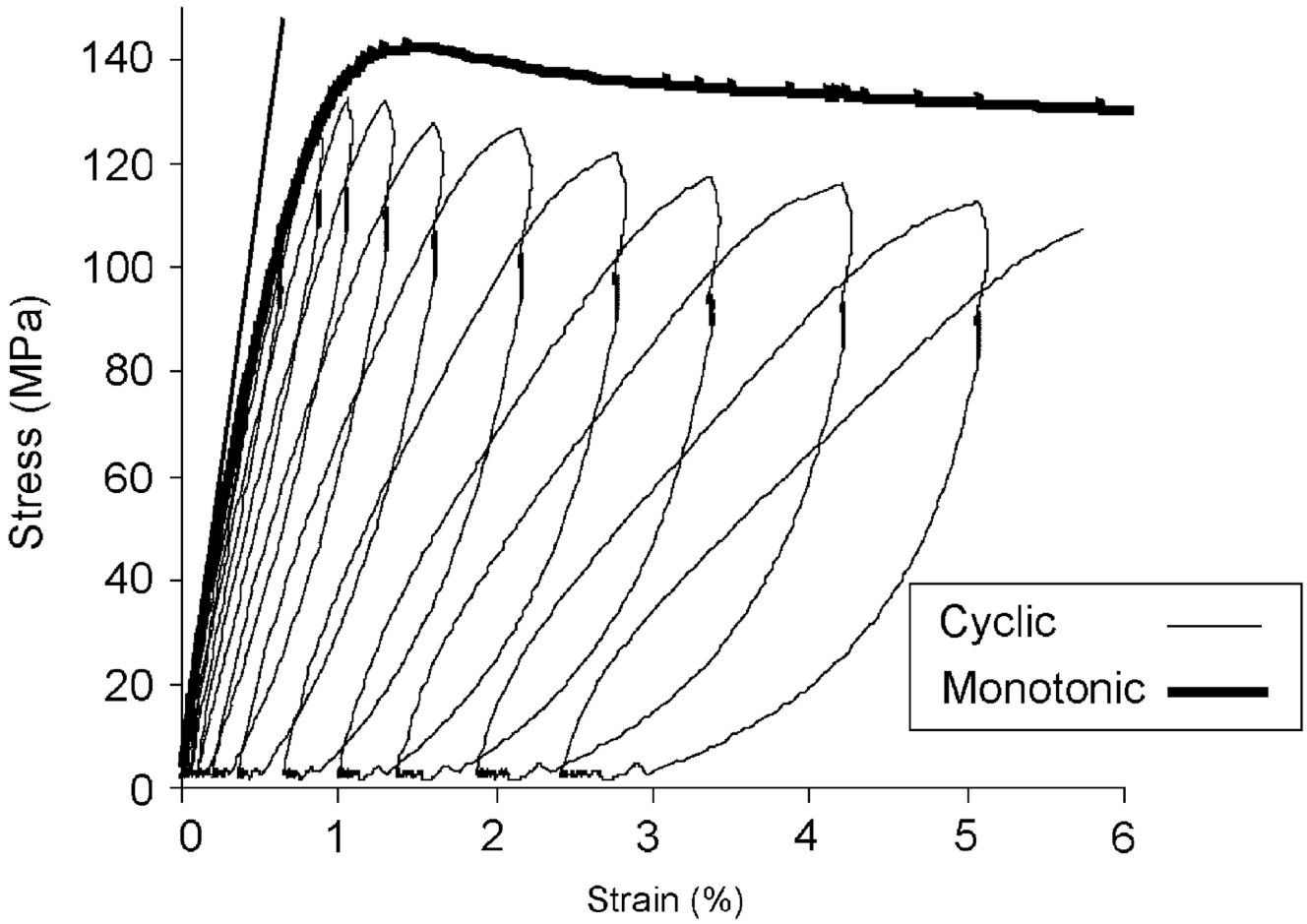

Fig. 4.
Comparison between the stress–strain curve of monotonic loading test and the envelop of the stress–strain curve of the progressive cyclic loading test on bone specimens from the same donor.

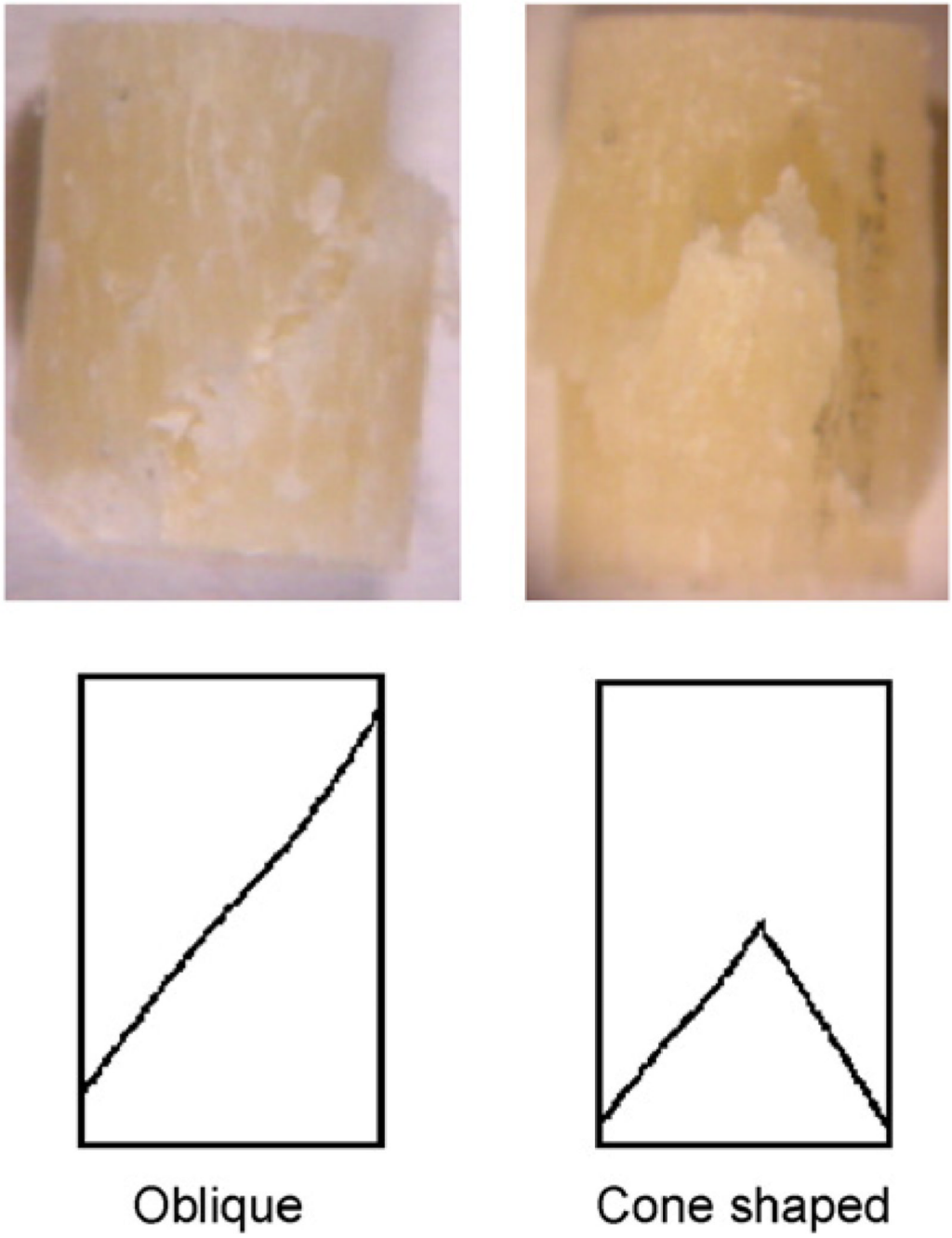

Fig. 5.
Photographs of two typical failure patterns observed among the compressed specimens: oblique fracture and cone-shaped fracture.

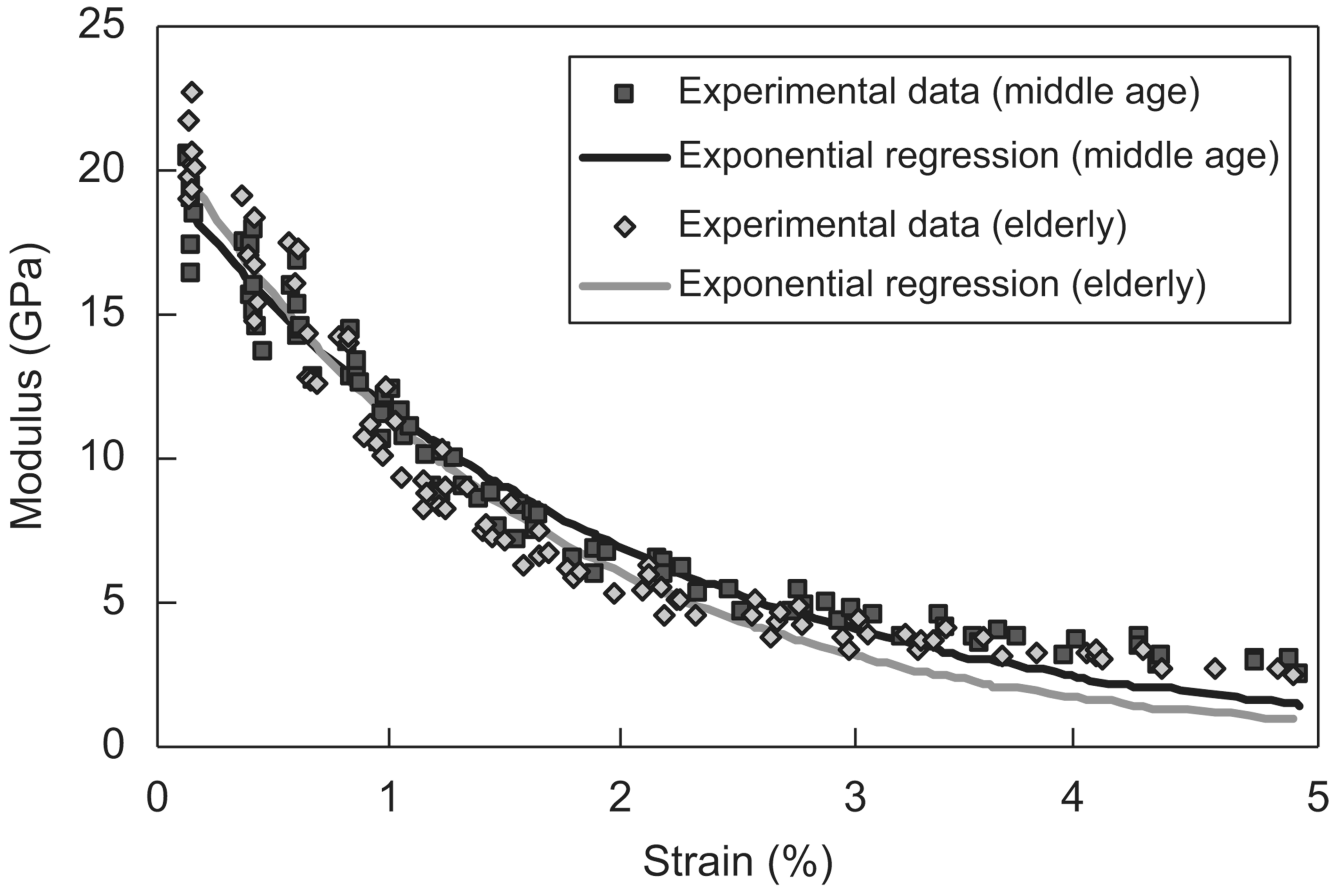

Fig. 6.
Relationship between the instantaneous modulus and applied strain and the exponential regression fitting of the curves for middle-aged ($E_i = 18.8e^{-52.7(\varepsilon_i - 0.0012)}$, $R^2 = 0.96$) and elderly ($E_i = 19.0e^{-64.3(\varepsilon_i - 0.002)}$, $R^2 = 0.95$) groups. The value of m is greater for elderly bone ($m = 64.3$) than middle-aged bone ($m = 52.7$), suggesting a faster modulus loss for elderly bone.

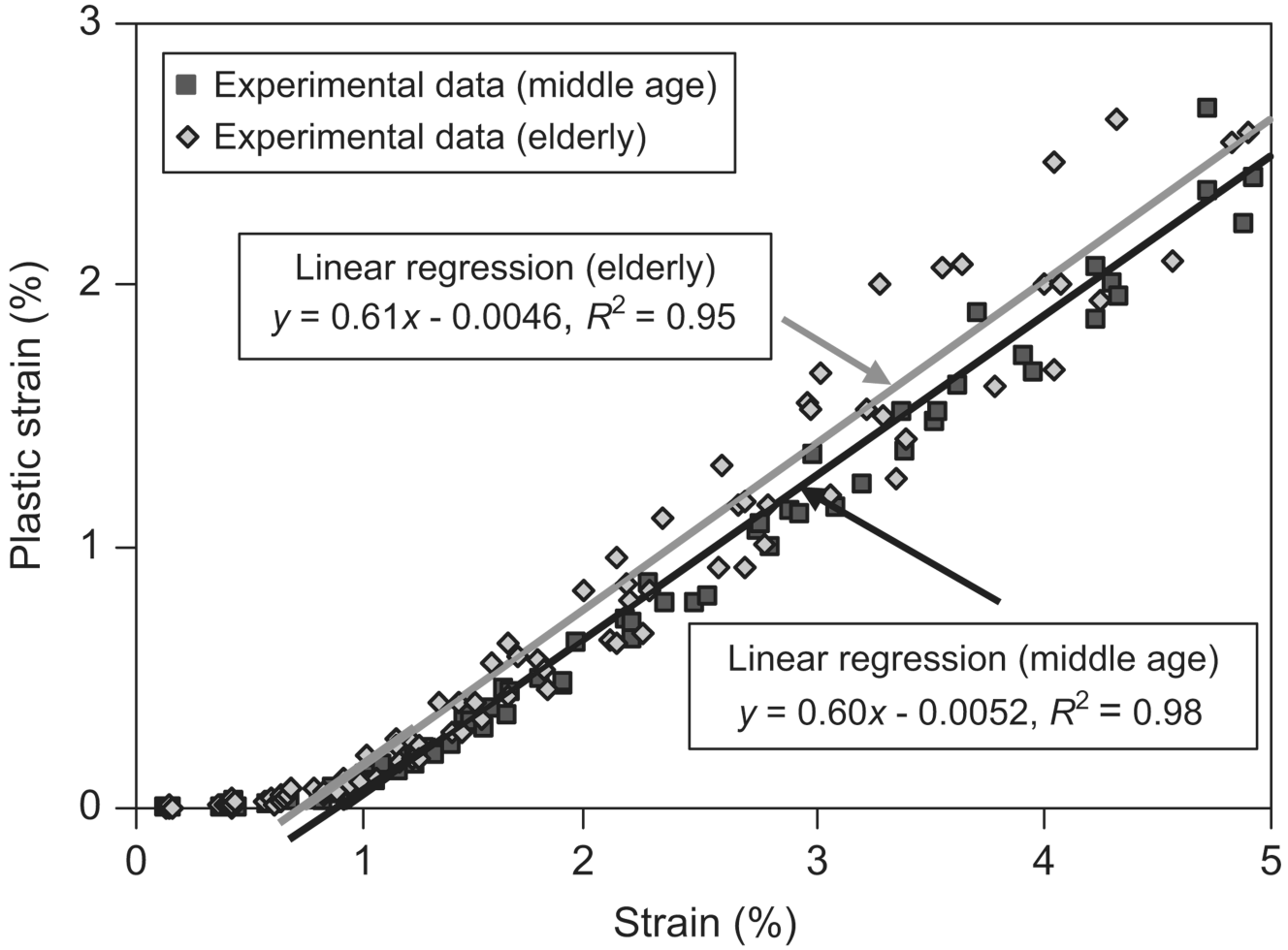

Fig. 7.

Relationship between the plastic strain (ε_p) and the applied strain (ε_i) and the linear regression fitting of the linear part of the curves for both middle-aged ($\varepsilon_p = 0.60\ \varepsilon_i - 0.0052$, and $R^2 = 0.98$) and elderly groups ($\varepsilon_p = 0.61\ \varepsilon_i - 0.0046$, and $R^2 = 0.95$). The yield strain (ε_y) is determined at the intersection of the regression line with the horizontal axis.

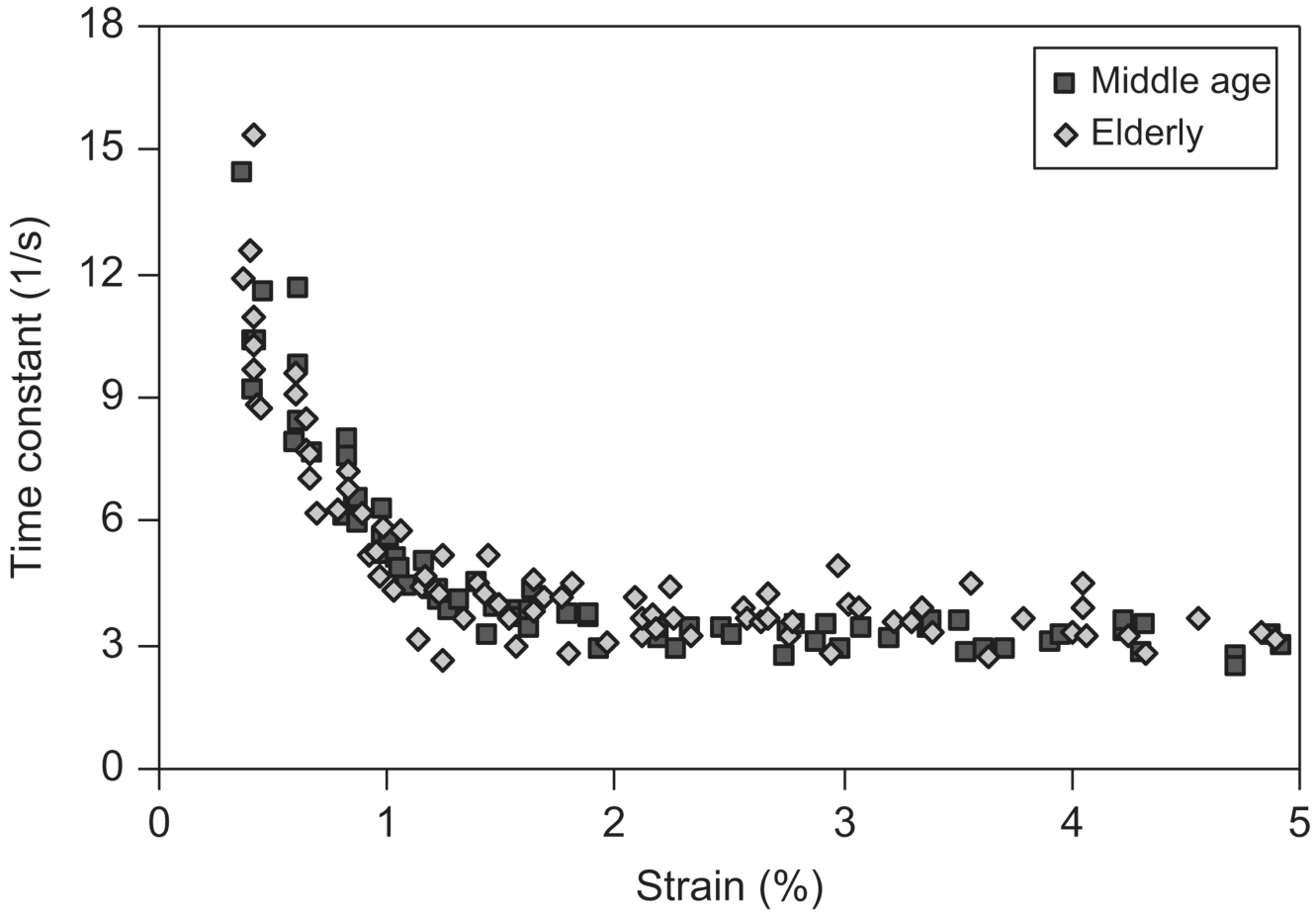

Fig. 8.
Relationship between the viscoelastic time constant (τ) and the applied strain (ε_i) for both middle-aged and elderly groups.

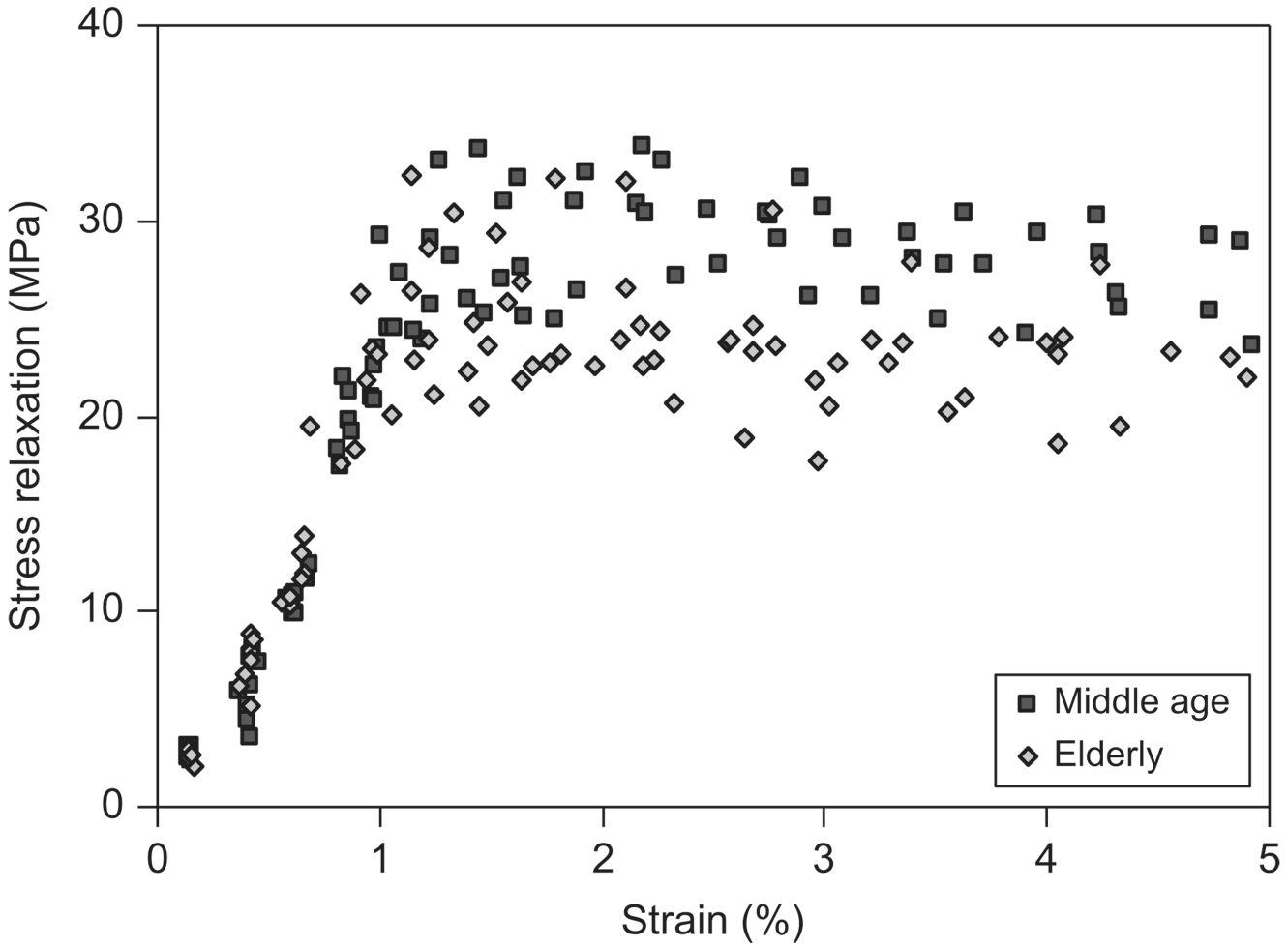

Fig. 9.
Relationship between the stress relaxation ($\Delta\sigma_0$) and the applied strain (ε_i) for both middle-aged and elderly groups.

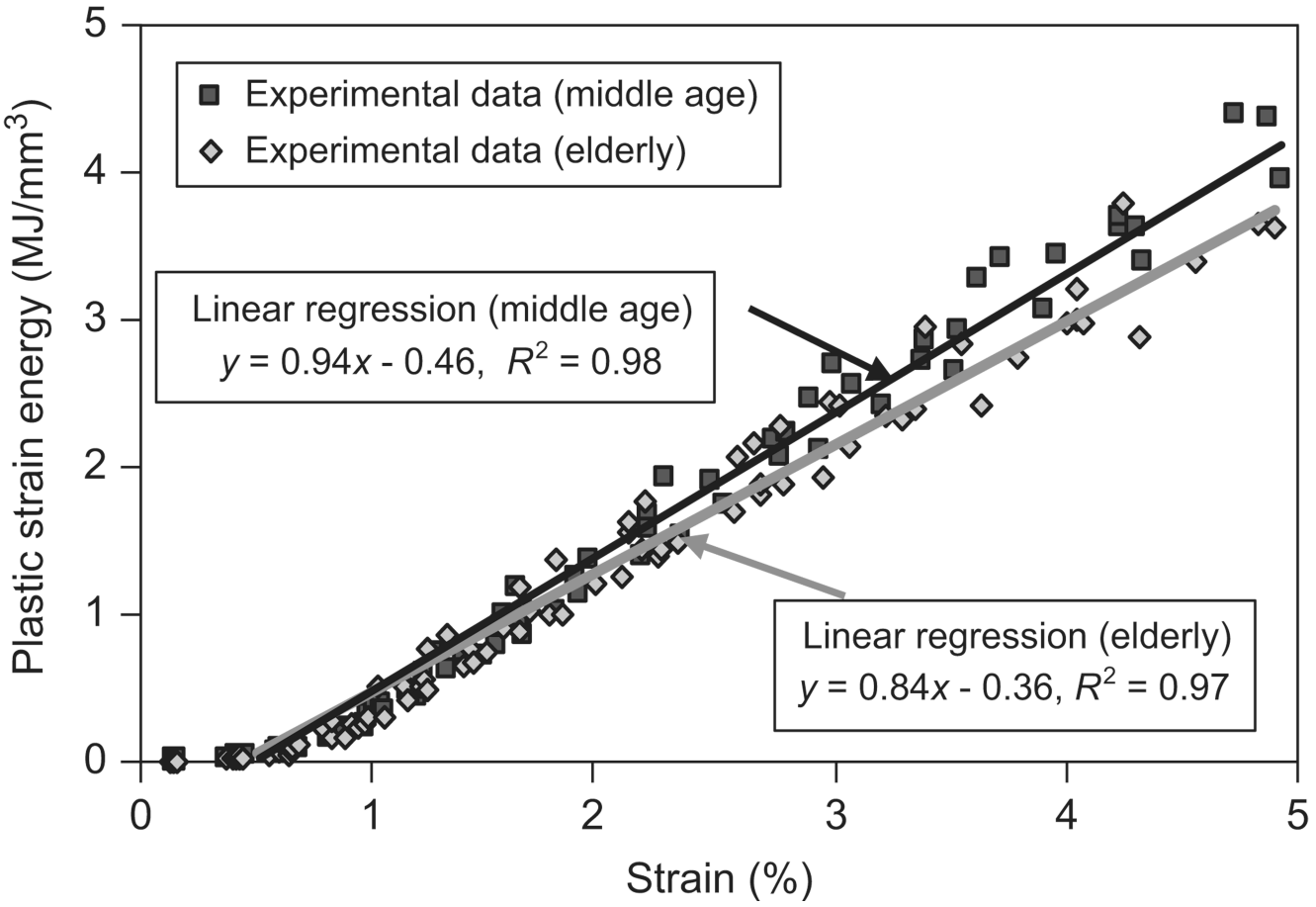

Fig. 10.
Relationship between plastic strain energy dissipation (*Upl*) and applied strain (ε_i) and the linear regression fitting of the curves for both middle-aged (R^2 = 0.98) and elderly groups (R^2 = 0.97).

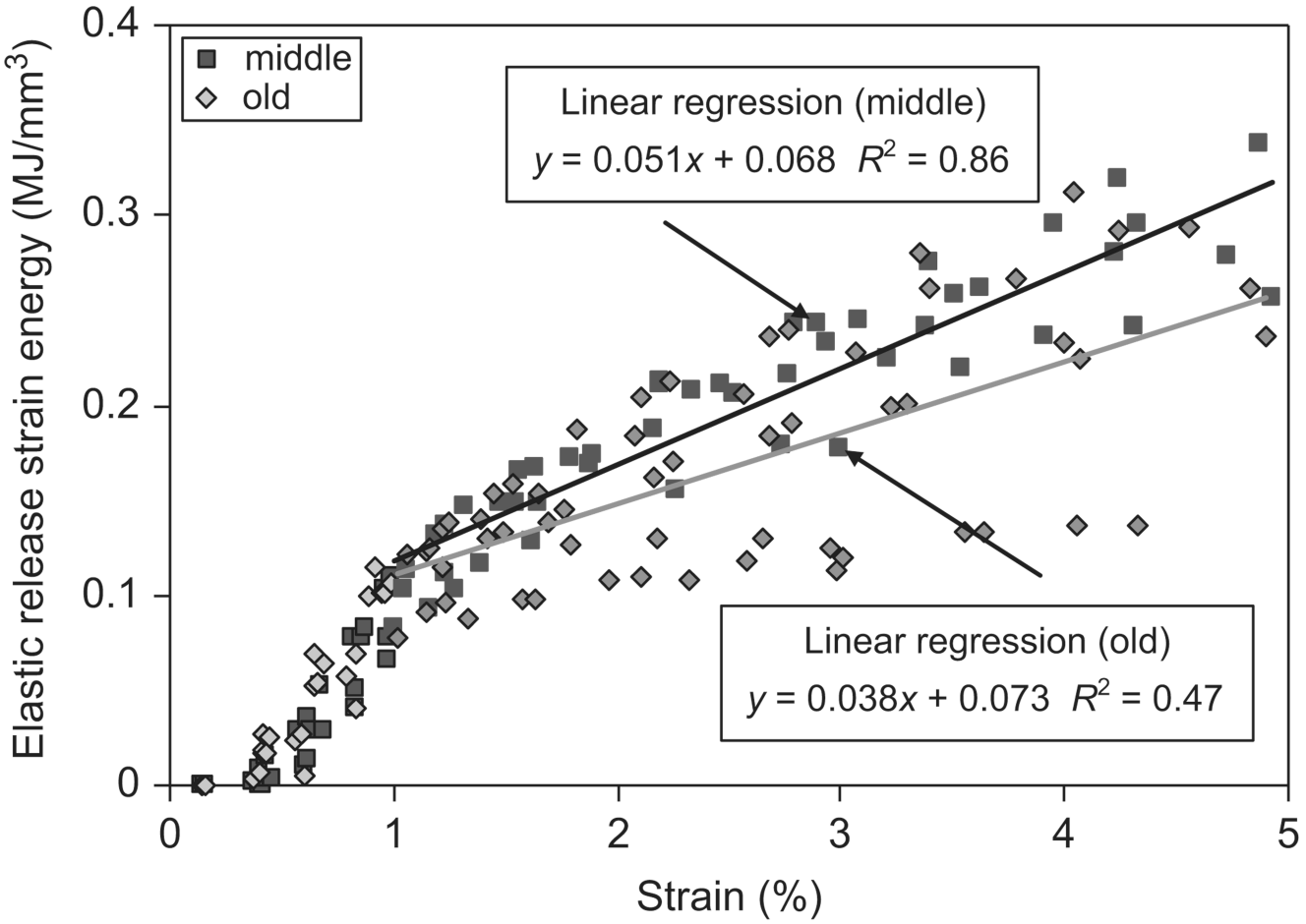

Fig. 11.
Relationship between elastic release strain energy dissipation (*Uer*) and the applied strain (ε_i) for both middle-aged and elderly groups. Linear regression was applied in the region with strain more than 1%.

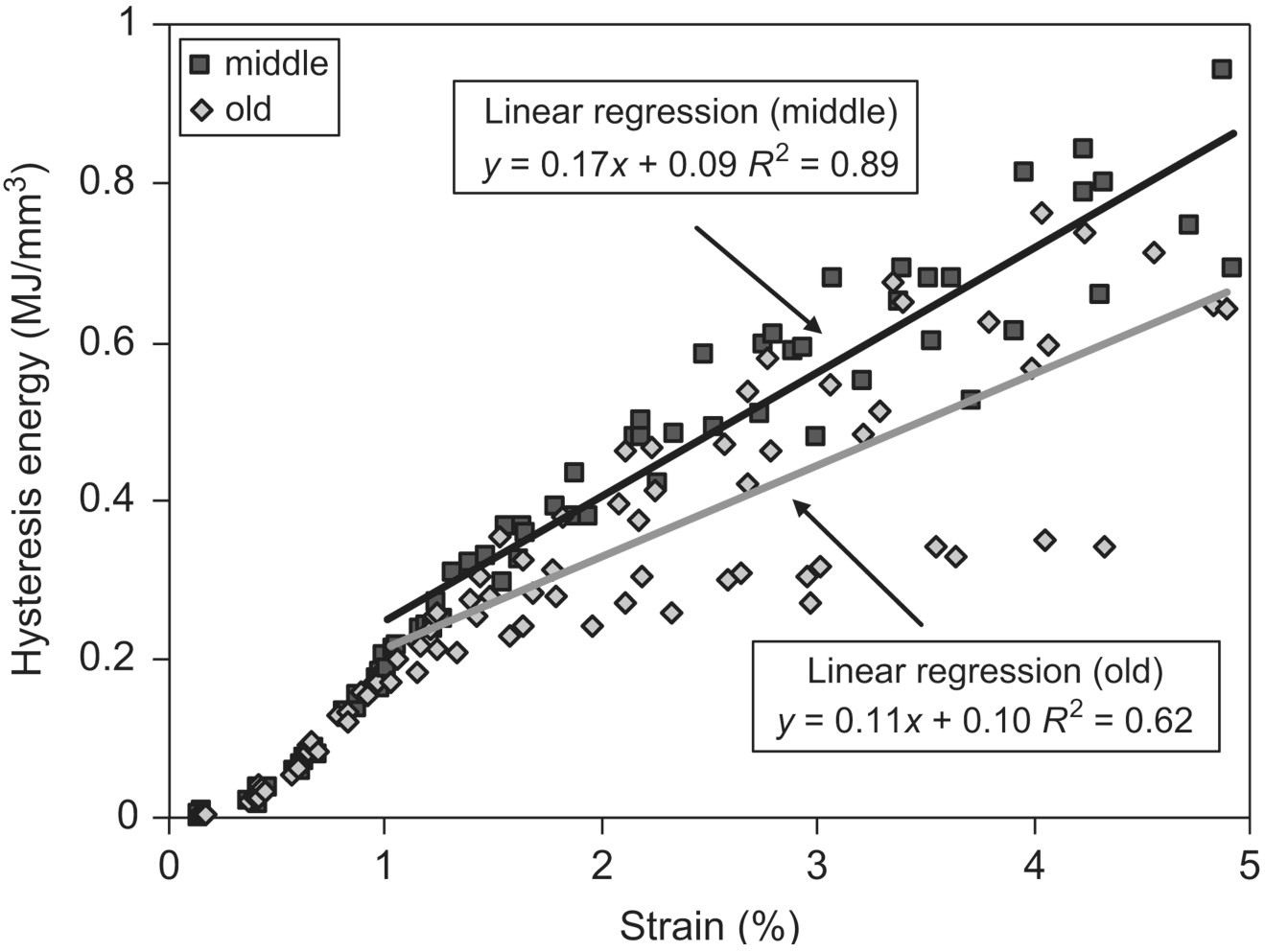

Fig. 12.
Relationship between hysteresis energy dissipation (*Uhy*) and the applied strain (ε_i) for both middle-aged and elderly groups. Linear regression was applied in the region with strain more than 1%.

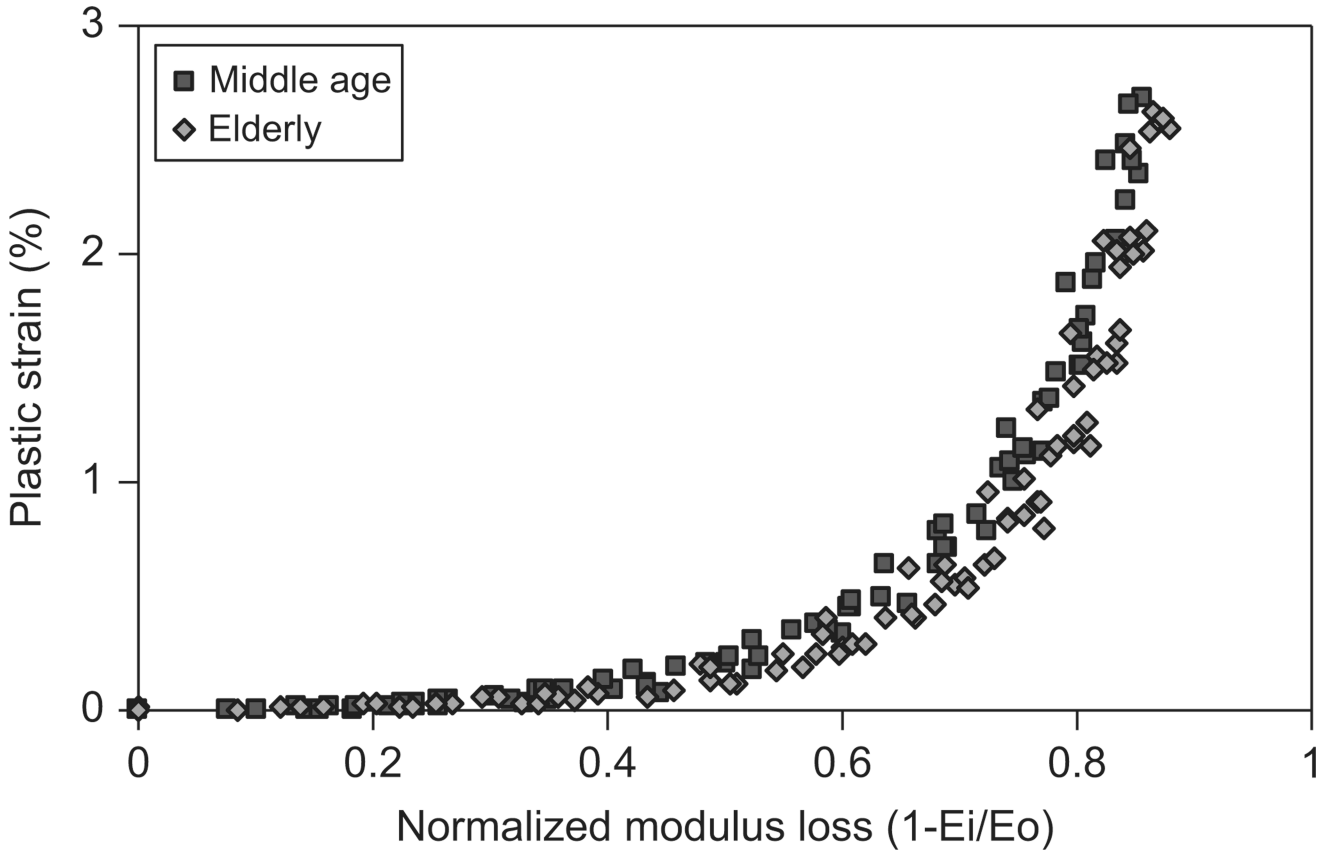

Fig. 13.
Relationship between the plastic strain (ε_p) and modulus loss (= $1-E_i/E_0$) for both middle-aged and elderly groups.

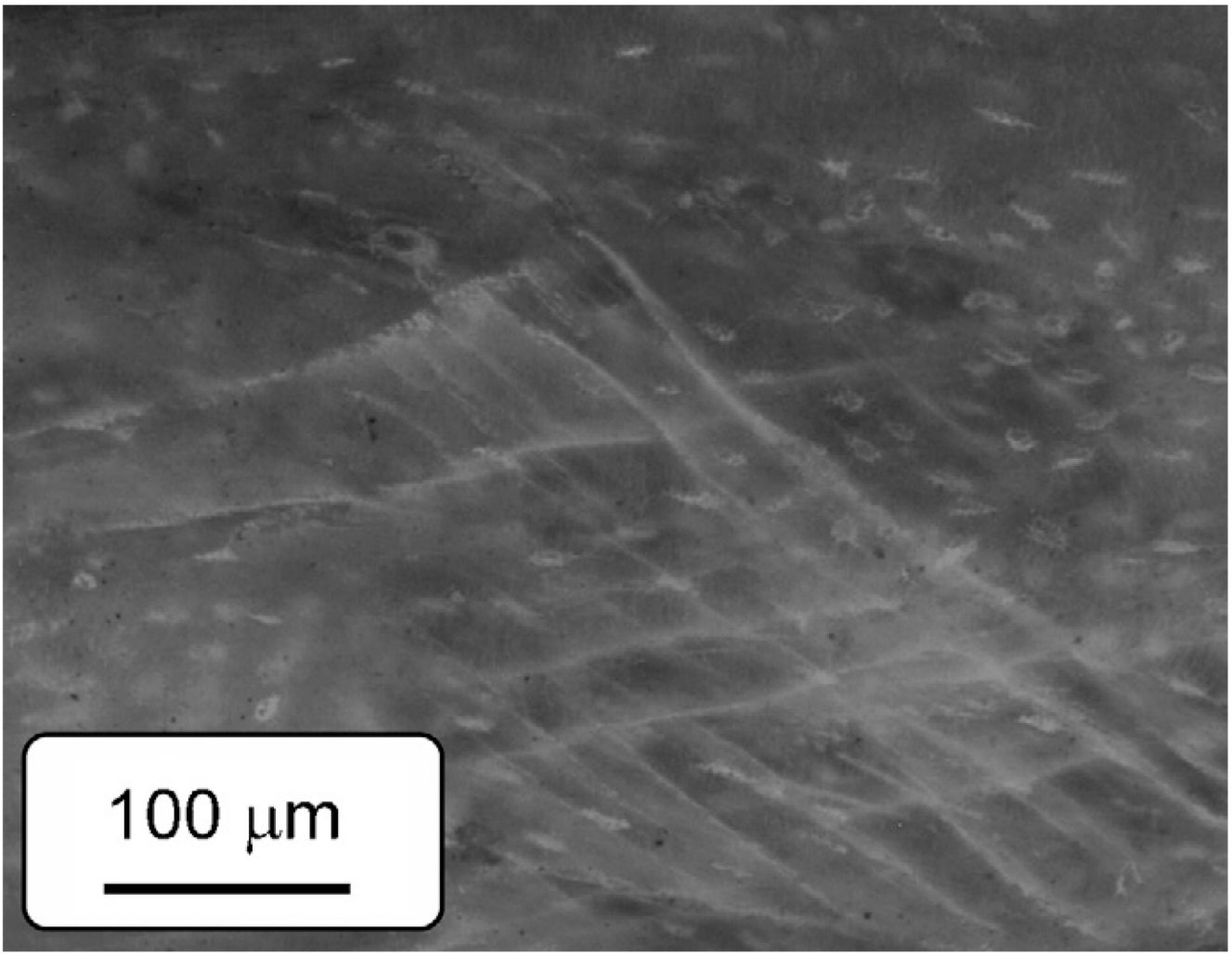

Fig. 14.
Fluorescence image of a damaged zone of bone in compression stained in basic fuchsin. Cross-hatched microcracks oriented in the directions of the maximum shear stress are observed.

Table 1

Comparison of bulk tissue properties between the two age groups.

	Group comparison		
	Middle-aged	**Elderly**	**Student's *t*-test**
E_0 (GPa)	19.1 ± 1.03	20.4± 1.27	$p = 0.06$
ε_y(%)	0.820 ± 0.0340	0.711 ± 0.0749	$p = 0.02$
σ_y (MPa)	118 ± 9.49	107 ± 15.7	$p = 0.03$
σ_{ult} (MPa)	132 ± 8.62	122 ± 14.0	$p = 0.06$